ISSN 1392 - 1207. MECHANIKA. 2012 Volume 18(4): 461-466

PRI (palm rotation indicator): A metric for postural stability in dynamic nonprehensile manipulation

Borhan Beigzadeh*, Ali Meghdari, Saeed Sohrabpour*****
**School of ME, Iran University of Science and Technology, Tehran, Iran, E-mail: b_beigzadeh@iust.ac.ir*
***CEDRA, ME Department, Sharif University of Technology, Tehran, Iran, E-mail: meghdari@sharif.edu*
****CEDRA, ME Department, Sharif University of Technology, Tehran, Iran, E-mail: saeed@sharif.edu*

crossref http://dx.doi.org/10.5755/j01.mech.18.4.2324

1. Introduction

Object manipulation is a main category of robotics. In traditional form of manipulation problems, the main goal is to grasp an object using an articulated hand (usually with fingers) attached to a manipulator and then manipulate it with the corresponding manipulator. In such problems, one deals with complicated mathematical formulation to model the fingers grasping the object. Several concepts should be taken into account; stability of the grasp with special notice to the frictional issues and force– and form–closure conditions must be studied. The manipulation is then done in a quasistatic manner as accelerated motion of the object changes the stability conditions of the grasp. By taking advantage of dynamical behavior of the object while manipulated, a new window is opened to object manipulation, namely dynamic object manipulation. Dynamic object manipulation (it is also called Dynamic Nonprehensile Manipulation (DNM) meaning manipulation without grasping the object), however, simplifies the structure of manipulators while adding complexity to the control strategy, dynamical modeling, and stability analysis of the process. Pushing [1, 2], rolling [2], sliding [2], throwing [4,5], catching [4,5], batting [6], and so on, are the concepts based on which dynamic object manipulation is usually performed.

DNM of a multibody object [7], however is a kind of dynamic manipulation during which a passive or active, multilink object is subject to manipulation. In [7], we did such manipulation using a series of manipulators. Postural stability which is a key factor in doing such manipulation is evaluated using a reference point, namely Palm Rotation Indicator (PRI), introduced here. Moreover, the relation of such point to other metrics of postural stability in biped locomotion such as Zero moment point (ZMP) is studied here.

2. Dynamic nonprehensile manipulation of multibody objects

The problem discussed here is a kind of DNM process. In this process, we use a series of planar m-link manipulators to manipulate multibody n-link objects. Each manipulator, i.e. k-th manipulator, has a flatted end-effector S_M, i.e. S_M^k , which plays the role of contact surface during the manipulation. Moreover, we simply assume that each kind of objects has two contact surfaces, namely S_1 and S_2; Fig. 1. These contact surfaces will be alternatively in contact with the manipulators' contact surfaces during the manipulation process.

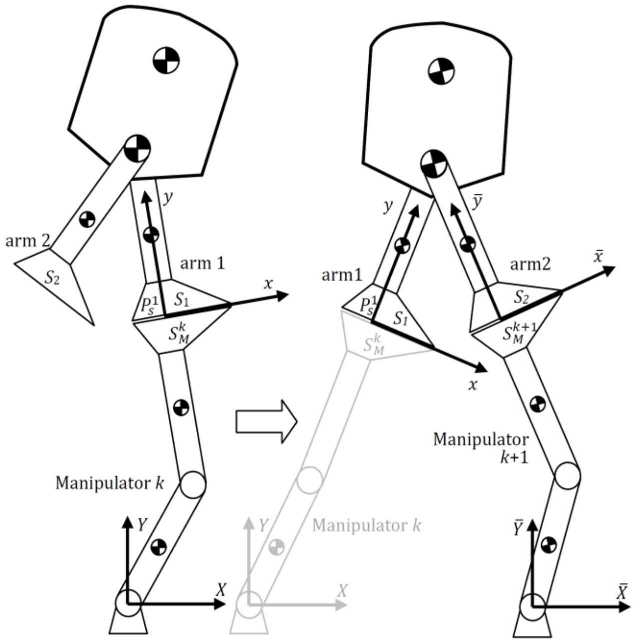

Fig. 1 Contact phase (left), impact phase (right)

During manipulation, by our definition, the cycle k is a part of the manipulation process which starts at time τ_k with the impact of one contact surface with the end-effector of manipulator k and finishes at time τ_{k+1} with the impact of the other contact surface with the end-effector of the manipulator $k + 1$. More precisely, a cycle begins just before one impact, and ends just before the next impact. Therefore, each cycle can be divided into two separate phases with no overlap: Impact Phase and Contact Phase. The manipulation process is then a series of such cycles. The impact phase is an instantaneous phase changing velocities of the system suddenly, but leaving the positions unchanged. In fact, the manipulation process is wholly a contact phase with some impulse effects. The contact phase is then defined when arm 1 is in contact with end-effector k (k = 1, 2, 3, …). That is, S_1 lies exactly on S_M^k with no slippage or separation (postural stability); see

Fig. 1. By this assumption, it is reasonable to consider that the sliding joint between contact surfaces acts as a fixed joint and therefore we may assume that arm 1 and end-effector k are a united part in a new object-manipulator system during the successful cycle k. This way other aspects of the process such as dynamics and control could be simply dealt with. However, postural stability is the key factor in this direction. Anyway, the governing equation of the system is:

$$\left.\begin{aligned} \dot{\boldsymbol{x}} &= f(\boldsymbol{x}) + g(\boldsymbol{x})u & \boldsymbol{x} \notin S \\ \boldsymbol{x}^+ &= \Delta(\boldsymbol{x}^-) & \boldsymbol{x} \in S \end{aligned}\right\} \tag{1}$$

where $\boldsymbol{x} = \left[\boldsymbol{q}^T, \dot{\boldsymbol{q}}^T\right]^T$, $\boldsymbol{q} \in \Re^{n+m-1}$ is the generalized variables of the system, + and – signs corresponds to just after and before impact. Also

$$f(\boldsymbol{x}) = \begin{bmatrix} \boldsymbol{q} \\ -\boldsymbol{M}^{-1}(\boldsymbol{C}\boldsymbol{q} + \boldsymbol{G}) \end{bmatrix}, \ g(\boldsymbol{x}) = \boldsymbol{M}^{-1}\boldsymbol{B} \tag{2}$$

$\boldsymbol{M}$ and $\boldsymbol{C}$ are, respectively, $m + n - 1$ square matrices and $\boldsymbol{G}$, $\boldsymbol{u} \in \Re^{n+m-1}$ (see [7] for details). Furthermore

$$S = \left\{\boldsymbol{x} \mid E(\boldsymbol{x}) = 0, \boldsymbol{q} \in (0, 2\pi)^{n+m-1}, \dot{\boldsymbol{q}} \in \Re^{n+m-1}\right\} \tag{3}$$

$E(\boldsymbol{x})$ is any function of $\boldsymbol{q}$ whose vanishing indicates the reaching of S_1 to the end-effector $k + 1$, e.g. the distance between them.

3. Postural stability in DNM: PRI point

Based on our definition, postural stability means that the contact conditions during contact phase and impact phase must not be violated. That is, no slip and no rebound conditions should be satisfied in order that the process has postural stability. To evaluate it, we define a metric point, namely PRI, indicating whether the palm of object would rotate with respect to the contact surface S_M^k. In fact, the point on the contact surface S_1 where the net reaction force of the manipulator acts without any torque is the PRI point.

During contact phase, for a given trajectory, it is possible to write the position of the object's center of mass, $\boldsymbol{P}_O^{CM}$ as a function of $\boldsymbol{q}$, $\Psi(\boldsymbol{q})$. So for its velocity and acceleration, $\boldsymbol{v}_O^{CM}$ and $\boldsymbol{a}_O^{CM}$, we have

$$\left.\begin{aligned} \boldsymbol{v}_O^{CM} &= \frac{\partial \Psi}{\partial \boldsymbol{q}}\dot{\boldsymbol{q}} \\ \boldsymbol{a}_O^{CM} &= \dot{\boldsymbol{q}}^T \frac{\partial^2 \Psi}{\partial \boldsymbol{q}^2}\dot{\boldsymbol{q}} + \frac{\partial \Psi}{\partial \boldsymbol{q}}\ddot{\boldsymbol{q}} \end{aligned}\right\} \tag{4}$$

then we may simply write

$$\boldsymbol{F}_c^1 = M_O \boldsymbol{R}\left(\boldsymbol{a}_O^{CM} - \boldsymbol{g}\right) \tag{5}$$

where $\boldsymbol{R}$ maps $\boldsymbol{a}_O^{CM}$ from inertial frame to the local frame x–y attached to the end-effector k; see

Fig. 1. It is notable that the effect point of $\boldsymbol{F}_c^1$ is P_s^1 which is simply the intersection of the contact surfaces direction and the line connecting the last joint of the manipulator k and the first joint of arm 1; see

Fig. 1 and Fig. . Because we assume that the contact surfaces compose a fixed joint, there is a couple acting on S_1 in addition to $\boldsymbol{F}_c^1$, namely $\boldsymbol{M}_c^1$, which could be written using the equation of moment of the system about the manipulator's base

$$\boldsymbol{M}_c^1 = \dot{\boldsymbol{H}} - P_s^1 \boldsymbol{R}^T \boldsymbol{F}_c^1 \tag{6}$$

Now the distance of PRI from P_s^1 can be obtained from

$$d_{PRI} = \boldsymbol{M}_c^1 \boldsymbol{e}_z / \boldsymbol{F}_c^1 \boldsymbol{e}_y \tag{7}$$

Thus, the no slip and no rebound conditions are

$$-d_l < d_{PRI} < d_r \tag{8}$$

$$\boldsymbol{F}_c^1 \in \aleph \tag{9}$$

where d_l and d_r are the left and right distance of P_s^1 from palm edges and $\aleph$ is the vector set including all vectors lying in the friction cone (Fig. 2)

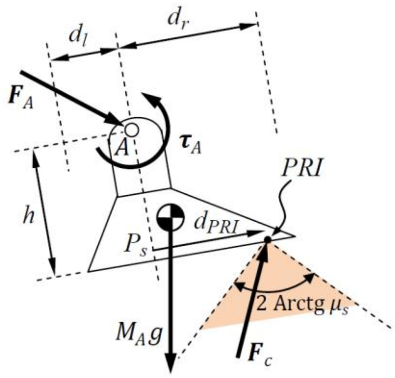

Fig. 2 Contact surface, PRI point, friction cone, and loads acting on ankle of arm 1

4. Illustrative examples

As we stated before, the DNM systems, which we described, could be passive or active. Therefore, two examples are chosen to be studied here one of which is the manipulation of an octagonal object using simple, passive, 1 DOF manipulators (Fig. 3) and the other is a DNM problem dealing with manipulation of a 3-link, active object using a series of 2-link active manipulators (Fig. 1). In both systems we study the postural stability of the systems using PRI analysis.

4.1. Manipulation of octagonal object

In this example, each manipulator has point-mass in its end-effector. Moreover, the object has homogeneously distributed mass of M with the moment of inertia (I) about its COM. Other parameters can be seen in Fig. 3.

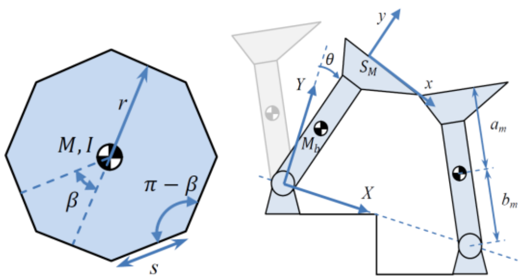

Fig. 3 Octagonal object and passive, 1-DOF manipulators

Following the procedure described in this paper, we model the problem of passive manipulation of a polygonal object. In the contact phase, the DOF of the total system is one. That is, the configuration of the whole system is unique for an arbitrary value of the joint angle of the manipulator. Then we have

$$\left.\begin{aligned} \boldsymbol{M} &= \left[M_b b^2 + I + MR^2\right] \\ \boldsymbol{C} &= [0] \\ \boldsymbol{G} &= \left[-\left(M_b b + MR\right) sin\left(\gamma + \theta\right) g\right] \end{aligned}\right\} \tag{10}$$

where $R = a + b + r$. For the impact phase, we can easily derive the transition model as

$$\boldsymbol{x}^+ = \begin{bmatrix} \theta^+ \\ \dot{\theta}^+ \end{bmatrix} = \begin{bmatrix} -1 & 0 \\ 0 & \dfrac{MR^2 \cos\beta + I}{MR^2 + M_b b^2 + I} \end{bmatrix} \boldsymbol{x}^- \tag{11}$$

These two models determine exactly the dynamic behavior of the system in both contact and impact phases.

Table 1
Parameters corresponding to Passive manipulation of an octagonal object

R	***β***	***a***	***b***	***M_b***	***M***	***I***	***g***	***γ***
0.25 m	45 deg	0.4 m	0.6 m	1 kg	10 kg	1 kg m^2	9.8 m/s^2	5 deg

Table 2
Parameters corresponding to manipulation of a 3-link object using 2-link manipulators

Object's Parameters							
L_A	L_O	s	a	b	m	Mj	M_O
0.5 m	0.25 m	0.1 m	0.05 m	0.05 m	0.5 kg	2 kg	5 kg

Manipulators' Parameters			
L_m	L_{mb}	M_m	M_{mb}
0.5 m	0.5 m	0.1 kg	0.5 kg

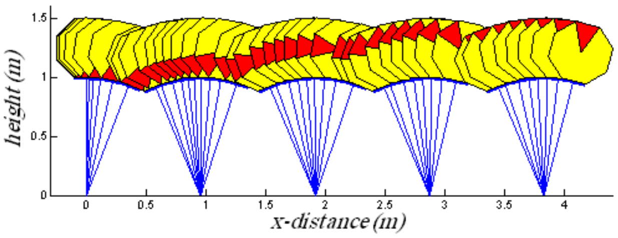

Fig. 4 Snapshots of manipulation of an octagonal object

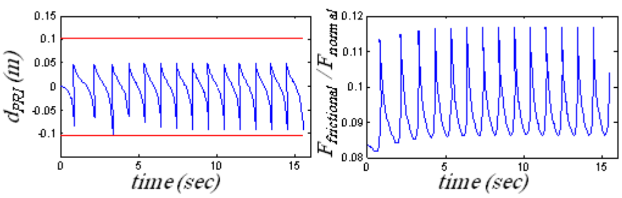

Fig. 5 PRI and ratio of frictional force to normal force in the first example

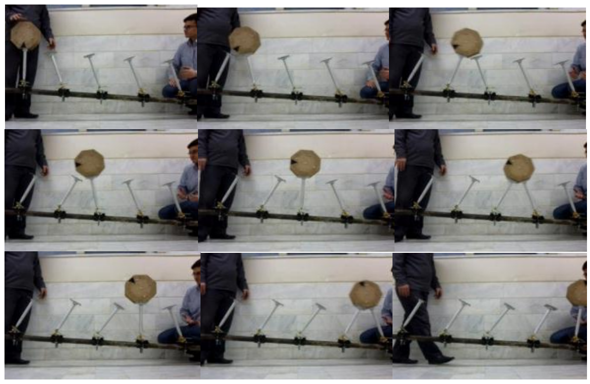
Fig. 6 Experimental implementation of passive manipulation of octagonal object

Having simulated the process we can easily see that if the PRI is inside the convex hull of the contact surface of the object, then the process is performed stably; in this example $d_r = -d_l = s/2$ and parameters of the object and manipulators are listed in Table 1. Some snapshots of the process are depicted in Fig. 4 while the diagram of is d_{PRI} plotted versus time in Fig. 5. Also, Fig. 5 shows that for friction coefficient less than 0.12, the object does not slip with respect to the manipulators. Experiments also verify the simulation results; Fig. 6 illustrates that our mechanism (the name is Gaam-Gard) which is an experimental implementation of this example, performs the process without any failure.

4.2. Manipulation of 3-link, active objects

In this example, we use a 2-link manipulator to manipulate a three-segment active object (see Fig. 1 for details). In this example, each manipulator is active. Therefore, the integrated manipulator/object system is a fully actuated system. All links' mass are concentrated in their COMs. The parameters for this example are as in Fig. 7 and Table 2. Without entering the control issues of the problem (appropriate strategies are discussed in [7]), we show the simulation results. Some frames of the process are illustrated in Fig. 8. In this example, the PRI point is inside the convex hull of the contact surface of the object. This can be seen in Fig. 9. In this figure, it is also shown that the ratio of the frictional force to the normal force acting on contact surface of the object which determines the limitation if the frictional coefficient is less than 0.4. That is, slip does not occur for the surfaces with frictional coefficient less than 0.4.

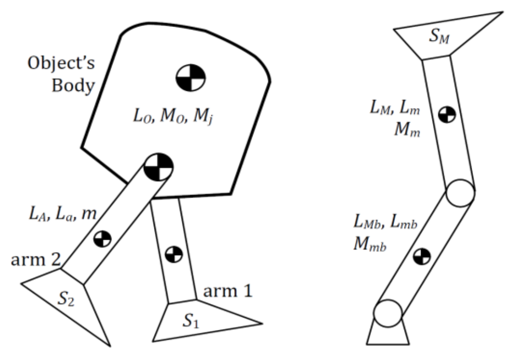

Fig. 2 Parameters of the object and the manipulators in manipulation of 3-link object using 2-link manipulators

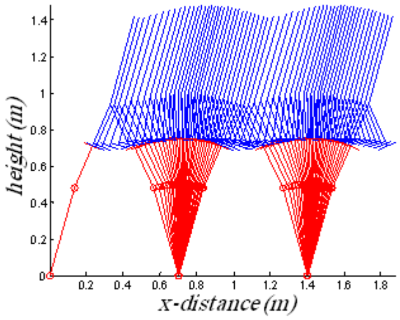

Fig. 3 Snapshots of manipulation of 3-link object

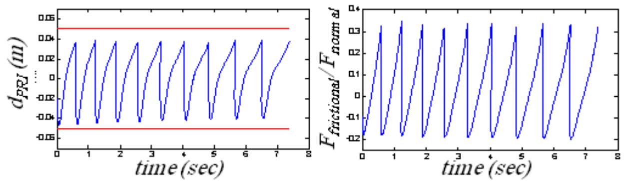

Fig. 4 PRI and ratio of frictional force to normal force in second example

5. Dynamic biped walking as a special case of DNM

There are close similarities between DNM and dynamic biped walking (DBW). There is a significant study in this regard in [4] where we have shown that DBM could be seen from the window of DNM. Here, we discuss that DBW is a special case of DNM problem which we defined in section 2. The concept of multibody object in this kind of manipulation covers a wide range of objects. For example, it is acceptable to assume that a rigid body object is a multibody one with zero internal DOF.

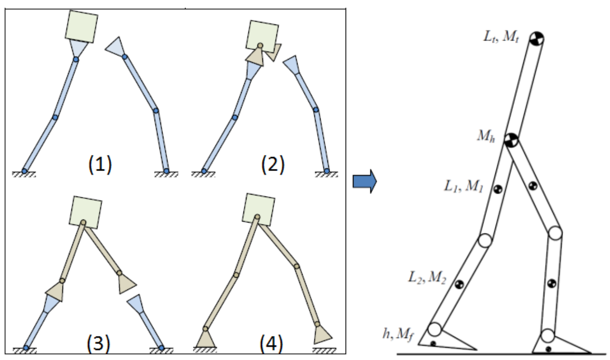

Fig. 5 Evolution of DBW from DNM (left) and parameters of the resulting biped (right)

See Fig. 10, 1. In this figure, DNM of a rigid-body object is depicted. Dealing with this kind of the problem includes considering dynamic stability issues in the presence of impact, while the control problem is not so complicated. In the next step, we simplify the structure of the individual manipulators by decreasing the number of links from 3 to 2; see Fig. 10, 2. Then the DOF of each manipulator will be 2. This indicates that two arms are added to the object. By the same procedure, we may construct a DNM system including manipulators with zero DOF and a two-arm object each of which has two links; Fig. 10, 4. As a result, the internal DOF of the object is 6 while the manipulators are, in fact, the same as the ground. That is, no actual manipulator could be detected in the problem. The phrase "manipulator" is used because the procedure from which we derived the problem was initially started from a DNM problem; actual manipulators can be seen in Figs. 10, 1-3. With a little investigation, it is apparent that the DNM system depicted in Fig. 10, 4 is a walking (more precisely, DBW) system. In fact, we look at the DBW as a DNM during which the biped robot is the object manipulated by the ground as a zero DOF manipulator. We then show that other aspects of the DBW could be seen from the window of DNM. In this paper, we specially discuss postural stability issues.

5.1. ZMP and FRI, special cases of PRI

Postural stability of a DBW system is analyzed by the concept of ZMP introduced by Vukobratovic in early nineties [8]. ZMP is defined as the point on the ground where the net moment of the inertial forces and the gravity forces has no component along the horizontal axes. For posturally stable locomotion, the necessary and sufficient condition is to have the ZMP within the support polygon at all stages of the locomotion gait [8]. Equivalently, FRI is a point on the foot-ground contact surface, within or outside the support polygon, at which the resultant moment of the force/torque acting on the foot is normal to the surface [9]. The difference between these two definitions is that the ZMP could not leave the footprint in the single-support phase, while the FRI could. We show that these two points are special cases of PRI in our defined nonprehensile manipulation problem. To do this, we focus on the arm 1 depicted in Fig. 2 and write the corresponding Euler equation about the manipulator's base. That is

$$\boldsymbol{M}_c^1 + \boldsymbol{\tau}_A + \boldsymbol{P}_s^1 \boldsymbol{R}^T \boldsymbol{F}_c^1 + \boldsymbol{P}_A^1 \boldsymbol{R}^T \boldsymbol{F}_A^1 + \boldsymbol{P}_{MA}^1 M_A \boldsymbol{g} = I_{zz}\alpha_A \boldsymbol{e}_z \qquad (12)$$

where $\boldsymbol{\tau}_A$ and $\boldsymbol{F}_A^1$ are the actuator torque and force acting on ankle, $\boldsymbol{P}_A^1$ is the ankle's position vector, $\boldsymbol{P}_{MA}^1$ is the position vector of the palm's COM, and M_A, I_{zz}, and α_A are the mass, angular momentum about the manipulator's base, and absolute angular acceleration, all corresponding to the palm. By computing $\boldsymbol{M}_c^1$ from Eq. (12) and $\boldsymbol{F}_c^1$ from Eq. (5), and then substituting in Eq. (7), we have

$$d_{PRI} = \frac{-\begin{pmatrix} \boldsymbol{\tau}_A + M_O \boldsymbol{P}_s^1 \left(\boldsymbol{a}_O^{CM} - \boldsymbol{g}\right) + \\ + \boldsymbol{P}_A^1 \boldsymbol{R}^T \boldsymbol{F}_A^1 + \boldsymbol{P}_{MA}^1 M_A \boldsymbol{g} \end{pmatrix} \boldsymbol{e}_z + I_{zz}\alpha_A}{M_O \boldsymbol{R}\left(\boldsymbol{a}_O^{CM} - \boldsymbol{g}\right)\boldsymbol{e}_y} \qquad (13)$$

Thus, considering a DNM problem including a two-arm object and zero DOF manipulators (see Fig. 10, case (4)), the DOF of the object equals that of a biped with feet. In this case, the contact surface between the object and individual manipulators is moved to the ground. So the ankle of the arm 1 (equivalently, the ankle of the stance leg in biped), is motionless and it may be considered as base point for inertial frame. In this case, local *x*-*y* frame coincides with inertial *X*-*Y* frame; that is $\boldsymbol{R} = \boldsymbol{I}$ and $\boldsymbol{g} = -g\boldsymbol{e}_y$. Since the palm (or biped's foot) is motionless, $\alpha_A = 0$ and $\boldsymbol{P}_A^1 = 0$. With a little investigation, we may rewrite

Eq. (13) as

$$d_{PRI} = \frac{-\tau_A - M_O h\ddot{X}_O^{CM} + M_A X_{MA}^1 g}{M_O\left(\ddot{Y}_O^{CM} + g\right)} \tag{14}$$

which is exactly the definition of FRI.

5.2. Walking of a 7-link, flat-feet biped as a DNM problem

Here, we study the DBW of a 7-link, Flat-Feet biped using the procedure described in section 5. We then analyze the postural stability of it using the definition of PRI; it is notable that as discussed in section 5.1, in this case, PRI is reduced to FRI (or ZMP). Therefore, if PRI is inside the support polygon, then the walking process is posturally stable.

To construct the biped model, we again refer to the example studied in section 4.2. The system in that example is in fact the one which is seen in Fig. 10, 2. By procedure that we discussed in section 5, we evolve a biped model which is shown in Fig. 10, 4. Following the modeling procedure that we presented in section 2 and also in [7], we can easily derive the mathematical model of the biped. The only notable thing in this regard is that for path planning issues, we assume that the horizontal displacement of the hip is a linear function of time. Then, we design five other outputs as functions of hip displacement. These five outputs along with the first assumption compose six virtual constraints. By using of output zeroing, in fact we have design for a posture control which let the biped walks with a nearly constant, horizontal speed while maintaining the posture of the robot in a desired manner. The five constraints which we consider to be functions of hip displacement are:

1. the inclination of the torso is $\pi/30$ rad from the vertical axis;
2. the ankle of swing leg moves along a parabolic function of hip displacement with maximum height of 0.1 m;
3. the hip height from the stance ankle is 0.85 m;
4. the horizontal distances of two ankles from the hip are always mirror;
5. the stance foot is always horizontal.

This way, the above virtual constraints along with the first assumption, are solved to obtain the time-dependant values of joint orientations. Then, we could apply a feedback linearization method to force the biped satisfy the virtual constraints.

Table 3

Numerical parameters of the 7-link walker

L_t	L_1	L_2	h	S	M_t	M_h	M_1	M_2	M_f
0.6 m	0.45 m	0.45 m	0.1 m	0.2 m	15 kg	5 m	2 kg	5 kg	0.1 kg

With the parameters shown in Fig. 10 and listed in Table 3, the simulation of biped walking is performed and we see that the PRI point (here, it is ZMP) is always inside the foot print of the biped (Fig. 11). Therefore, we conclude that the process is posturally stable. Some snapshots of the process are depicted in Fig. 12.

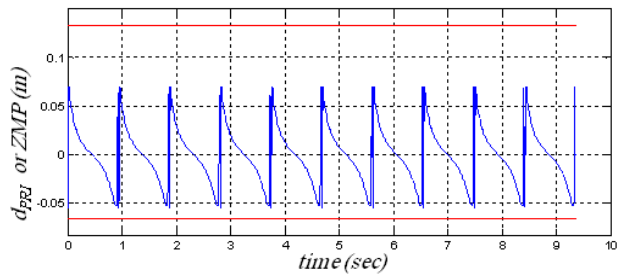

Fig. 11 PRI (or ZMP) corresponding to the biped walking

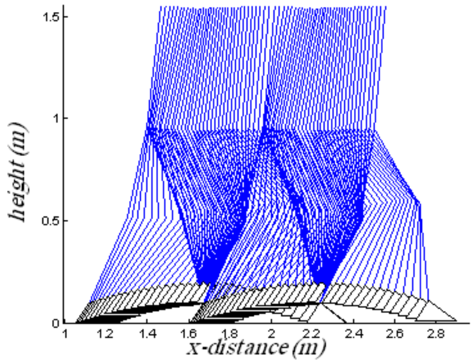

Fig. 12 Snapshots of biped's walking

6. Conclusion

In this paper, we briefly discussed a DNM system dealing with multibody objects. The postural stability of such process was taken into account and a corresponding metric point for stability, namely PRI, was introduced. Then we generally defined DBW as a special case of DNM; especially we proved that ZMP and FRI are special cases of PRI. Finally simulations and experimental implementations (in some cases), verified the results.

References

1. **Bernheisel, J.D.; Lynch K.M.** 2006. Stable transport of assemblies by pushing, IEEE Transactions on Robotics 22(4): 740-750. http://dx.doi.org/10.1109/TRO.2006.875488.
2. **Peshkin, M.A.; Sanderson, A.C.** 1988. The motion of a pushed, sliding workpiece, IEEE Journal of Robotics and Automation 4(6): 569-598. http://dx.doi.org/10.1109/56.9297.
3. **Alouges, F.; Chitour, Y.; Ruixing L.A.** 2010. Motion-planning algorithm for the rolling-body problem, IEEE Transactions on Robotics 26(5): 827-836. http://dx.doi.org/10.1109/TRO.2010.2053733.
4. **Beigzadeh, B.; AhmadAbadi, M.N.; Meghdari, A.; Akbarimajd, A.** 2008. A dynamic object manipulation approach to dynamic locomotion, Robotics and Autonomous Systems 56(7): 570-582. http://dx.doi.org/10.1016/j.robot.2007.11.002.
5. **Beigzadeh, B.; Meghdari, A.; Beigzadeh, Y.** 2007. Dynamic manipulation of objects using a series of manipulators, IMECE2007 (ASME), USA.
6. **Matsushima, M.; Hashimoto, T.; Takeuchi, M.; Miyazaki, F.** 2005. A learning approach to robotic table tennis, IEEE Transactions on Robotics 21(4): 767-771. http://dx.doi.org/10.1109/TRO.2005.844689.
7. **Beigzadeh, B.; Meghdari, A.; Sohrabpour, S.** 2010.

Control and manipulation of multibody objects, Proceedings of ASME-ESDA2010.
8. **Vukobratovic, M.; Borovac. B.** 2004. Zero-moment point - Thirty-five years of its life, International Journal of Humanoid Robotics 1(1): 157-173. http://dx.doi.org/10.1142/S0219843604000083.
9. **Goswami, A.** 1999. Foot rotation indicator (FRI) point: a new gait planning tool to evaluate postural stability of biped robots, ICRA1999 (IEEE) 1: 47-52.

B. Beigzadeh, A. Meghdari, S. Sohrabpour

DELNO SUKIMOSI INDIKATORIUS: PADĖTIES STABILUMO MATUOKLIS ESANT GRIEBIAMAJAM MANIPULIAVIMUI

R e z i u m ė

Straipsnyje aptariama padėties stabilumo problema esant griebiamajam sudėtingų objektų manipuliavimui. Kaip padėties stabilumo matuoklis naudojamas delno sukimosi indikatorius. Sistemos padėtis yra pastovi, jeigu delno sukimosi indikatorius yra objekto manipuliatoriaus išgaubto korpuso kontakto paviršiaus viduje. Manoma, kad dinaminis dviejų kojų judesys yra specialus griebiamojo manipuliavimo atvejis visais aspektais: įrodoma, kad ZMP (nulinio momento taškas) ir FRI (pėdos sukimosi indikatorius) yra specialaus delno manipuliatoriaus sukimosi atvejai. Nesudėtingų pavyzdžių imitavimo eksperimentai tyrimo rezultatus patvirtina.

B. Beigzadeh, A. Meghdari, S. Sohrabpour

PRI (PALM ROTATION INDICATOR): A METRIC FOR POSTURAL STABILITY IN DYNAMIC NONPREHENSILE MANIPULATION

S u m m a r y

In this study, we discuss the postural stability of a nonprehensile manipulation problem, which deals with multibody objects. As a metric for postural stability, we define PRI. Then, the system is posturally stable, if PRI is inside the convex hull of the object-manipulator contact surface. We then discuss that dynamic biped locomotion is a special case of dynamic nonprehensile manipulation in all aspects; we prove that ZMP (zero-moment point) and FRI (zoot rotation indicator) are special cases of PRI (palm rotation indicator). Simulations and experiments corresponding to simple examples support the results.

Keywords: palm rotation indicator, metric for postural stability, dynamic nonprehensile manipulation.

Received January 24, 2011
Accepted June 13, 2012